

FoldingBox: From 2D Layout to 3D Model???

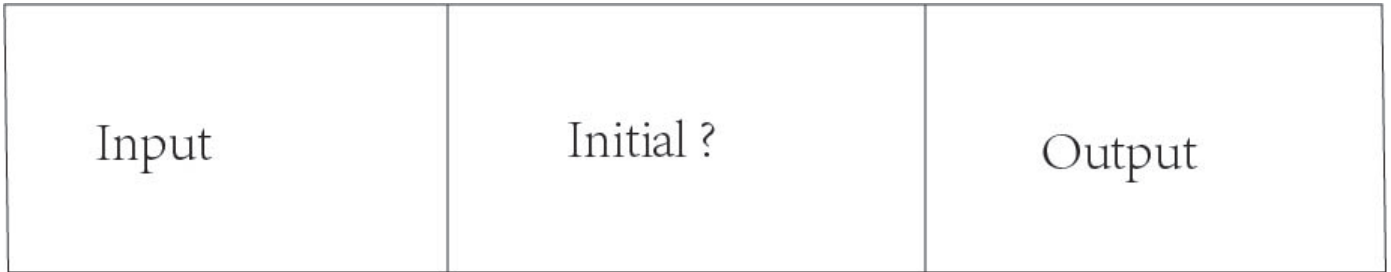


Figure 1: Overview. (a) A given input layout (b) XX (c) final 3D model generated by our methods

1 Abstract

In this paper, we will propose a new method for generating 3D models given its 2D layout, whose folded angles are learnt(?) by XX optimization.

Keywords: 3D Model?, XX

Concepts:

1 Introduction

Cartons have been widely used in packaging industry, to deliver various commodities including food items, daily necessities and electronic components. Instead of very basic packaging shapes like cubes, there exist multiple fantastic cartons to package wedding candies or take away coffee. These various designs increase much popularity, not to mention they're environment friendly due to their recycling and degradability.

Cartons are usually designed based on experience and trial-and-error? Depressingly, designers cannot see directly final model of carton when they are drawing its layout. Moreover, for non-experts, it's intractable to fold an irregular layout to final carton without instructions.

Researchers have studied paper folding problem for more than twenty years. It's been verified that given a net, i.e., a polygon and a set of creases, and the dihedral angles at each crease, we can know whether a polyhedron can be obtained in polynomial time. However, if the dihedral angles stay unknown, this problem becomes NP-hard even we simplify the 3D mdoel to orthogonal polyhedron whose dihedral angles are multiples of $\pi/2$ [Biedl et al. 2005].

However, the study above more focused on academic files, not on the applications of practical use.

Three-dimensional reconstruction has been wildly studied from different sources, such as point clouds, single images, and line drawings.

Permission to make digital or hard copies of part or all of this work for personal or classroom use is granted without fee provided that copies are not made or distributed for profit or commercial advantage and that copies bear this notice and the full citation on the first page. Copyrights for third-party components of this work must be honored. For all other uses, contact the owner/author(s). © 2017 Copyright held by the owner/author(s).

SIGGRAPH 2017 Posters, XX, 2017, XX, XX

ISBN: XX

DOI: XX

2 Related Work

Reconstrucion from single line drawings. Line drawings of three-dimensional objects have long been studied, and the main problem is still in reconstruction given projection on two-dimensional planes. Some researchers treat this task as optimization problem. [Marill 1991] proposed MSDA(Minimize the Standard Deviation of Angles) principle to emulate the interpretation of line drawings as 3D objects. This new criterion is used by many other researchers later. [Leclerc and Fischler 1992] combined MSDA with the deviation from planarity as objective terms. [Cao et al. 2005] added symmetry measure of the objects to get more complicated results. Some other researchers try to solve this problem from the information theoretic point of view. [Marill 1992] minimized the description length of objects based on the idea that we usually pick the simplest one from infinite possibilities when we see the line drawing. [Shoji et al. 2001] implemented the principle of minimizing the entropy of angle distribution between line segments using genetic algorithm. Different from the input above, ours are expanded layout of three-dimensional objects in 2D planes, the lackness of 3D topology is main concern in our problem.

Folding to polyhedron. [Lubiwi 1996] provided an dynamic programming algorithm based on Aleksandrov's theorem to test whether a polygon can be folded into polyhedra which takes $O(n^2)$ time and space. [O'Rourke 2000] examined three open problems on the subject of folding and unfolding. [Biedl and Gen 2004] has studied in polynomial time to solve the question of when is the graph orthogonally convex polyhedra given a graph, edge length and facial angles, also shown that it's NP-hard to decide whether the graph is orthogonally polyhedra or not. Rather than given graph, [Biedl et al. 2005] proved that if given a net along with the dihedral angle at each crease, we can know whether a net can be folded to a polyhedron in polynomial time, but it becomes NP-hard without the angles even adding constrains on orthogonal polyhedron, which results in more difficulties on more complex input. Later, [Demaine and O'Rourke 2010] proposed a survey on the folding and unfolding in computational geometry. Compared to our desired result, polyhedron is a set of polygons without overlap, nevertheless, our 3D model contains paste faces that needs to be fixed to another panel. These works above justify our problem being harder to solve causing by even intricker inputs.

Paper craft. Various types of paper crafts have been studied in the field of computing and mathmatics. Origami is the Japanese traditional paper art of making different kind of objects by a single sheet of paper, and has been long studied since 1970s [Kanade 1980]. Lately, there have been newly researched automatically generating a type of paper architecture named pop-ups. [Li et al. 2010]

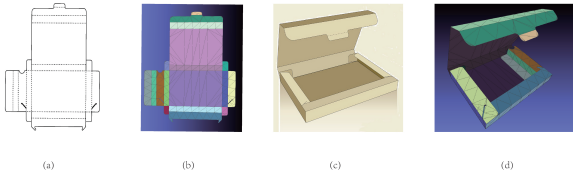


Figure 2: Given a design layout (a) and its 3D realization (c), we can approximately represent them by triangular mesh as (b) and (d).

presented formulation of layouts, sufficient conditions to generate foldable and stable paper architectures, and proposed an automatic algorithm given any 3D models. Plenty papers studied this subject following the idea of Li's and make new improvements[Li et al. 2011] [Ruiz et al. 2013] [Le et al. 2014].

Motion planning of paper folding.

3 Problem Formulation

In this section we present the general concept of our learning approach. The basic idea is to interpret the folded state of a box as a series of rotation angles along each edge, where the problem of predicting folded state is turned into a problem of predicting these angles.

3.1 Definitions and Notations

As an input to our method, we expect a 2D designed layout of a box represented as a flat triangular mesh L . As an output of our method, we deform the input triangular mesh into its 3D realization R , according to predicted angles along each of its edges.(An example is shown in Figure 2)

Without loss of generality, learning to predict the folded state of a box is learning an operator \mathcal{F} that maps every 2D layout to its 3D realization:

$$\mathcal{F} : \{L\} \rightarrow \{R\}, \quad (1)$$

in which $\{L\}$ is the set of all designed layout of boxes represented by 2D triangular meshes and $\{R\}$ is the set of 3D realization of the same boxes represented by deformed triangular meshes. A triangular mesh consists of a set of vertices, edges and faces $M = (V, E, F)$. The number of vertices, edges and faces varies from one mesh to another. However, a pair of (L, R) as the 2D layout and its corresponding 3D realization share the same topology and therefore they have the same number of vertices, edges and faces. A flat mesh as a 2D layout from $\{L\}$ has its z component of each vertex set to be a constant zero: $X_z(v) \equiv 0$ where $X = (X_x, X_y, X_z)$ is the vertex coordinate, and its normal of each face set as $(0, 0, 1)^T$: $n(f) \equiv (0, 0, 1)^T$, where $f \in F$.

3.2 From Shape Mapping to Functional Mapping

It is difficult to design a model and a learning scheme to learn the operator in Eq.(1). As we stressed before, the folded state of a box can be represented by a series of rotation angles along each edge which is why we can learn operator $\bar{\mathcal{F}}$ in (2) instead of \mathcal{F} in (1):

$$\bar{\mathcal{F}} : \{(F_0, F_1, \dots, F_n)\} \rightarrow \{\Theta\}, \quad (2)$$

in which the $\{(F_0, F_1, \dots, F_n)\}$ is a set of feature tensors that is extracted from $\{L\}$ to represent each 2D layout. A feature tensor is composed of n feature functions and a feature function has the form of $F_n : E \rightarrow \mathbb{R}$ which is a real value function that maps each

edge of a mesh to a real value. The $\{\Theta\}$ is a set of dihedral angle functions that maps each edge of a mesh to its angle of folded state. One dihedral angle functional has the form of $\Theta : E \rightarrow [0, 2\pi]$. To avoid ambiguity, we define the dihedral angle to be the one that the face normal pointed to.(need more elaboration with the definition of “positive dihedral angle”)

Unfortunately, it is still difficult to learn the operator $\bar{\mathcal{F}}$, since the dimension number of tensors and functions in $\{(F_0, F_1, \dots, F_n)\}$ and $\{\Theta\}$ varies from one pair of (L, R) to another.

To cope with this problem, we approximate each function as a linear combination of K basis functions $\Phi = \{\phi_k\}$ as $F_n \approx \sum \alpha_k \phi_k$ and $\Theta \approx \sum \theta_k \phi_k$. Each pair of (L, R) shares the same Φ , which allows us to further change the problem into learning $\hat{\mathcal{F}}$ as a mapping from the feature coefficient tensors to dihedral angle coefficients:

$$\hat{\mathcal{F}} : \{(\alpha_0, \alpha_1, \dots, \alpha_n)\} \rightarrow \{\{\theta_k\}\}. \quad (3)$$

3.3 Choice of Basis Functionals

We construct the basis functionals $\{\Phi\}$ as follows:

3.3.1 Method 1

Firstly, we construct the edge Laplacian matrix A for a mesh:

$$\begin{cases} a_{i,j} = w_{i,j} = \exp\left\{-\frac{d(e_i, e_j)}{\overline{d}(e_i, e_j)}\right\} \\ \text{if } i \neq j \text{ and } (e_i, e_j) \text{ shares a vertex.} \\ a_{i,i} = -\sum w_{i,j} \\ a_{i,j} = 0 \quad \text{otherwise} \end{cases} \quad (4)$$

in which the $d(e_i, e_j)$ is the euclidean distance between the centroids of the edge e_i and edge e_j and $\overline{d}(e_i, e_j)$ is the mean of $d(e_i, e_j)$ of edges that share a vertex on this mesh.

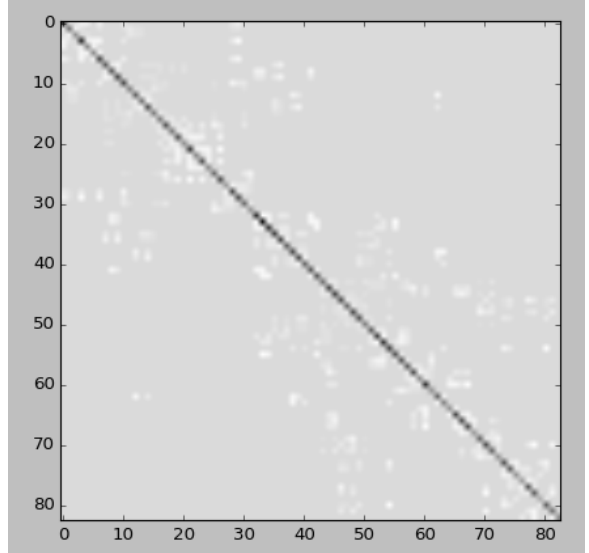


Figure 3: Laplacian matrix generated by method 1. Gray means value is 0, and the darker color is, the smaller value is.

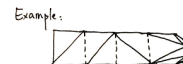
143 **3.3.2 Method 2**144 We can also construct the edge Laplacian matrix A' as

$$\begin{cases} a_{i,j} = w_{i,j} = \exp\left\{-\frac{d(e_i, e_j)}{d(e_i, e_j)}\right\} \\ \text{if } (e_i, e_j) \text{ are in the same face.} \\ a_{i,i} = -\sum w_{i,j} \\ a_{i,j} = 0 \quad \text{otherwise} \end{cases} \quad (5)$$

145 where we can remove the effect from little related edges.

146 **3.3.3 Method 3**147 Besides, we have another way to construct the edge Laplacian ma-
148 trix A'' focus on the folding edges $\{e_{f_i}\}$ as

$$\begin{cases} a_{f_i, f_j} = w_{f_i, f_j} = \exp\left\{-\frac{d(e_{f_i}, e_{f_j})}{\bar{d}(e_{f_i}, e_{f_j})}\right\} \\ \text{if } (e_{f_i}, e_{f_j}) \text{ satisfy condition 1.} \\ a_{f_i, -1} = a_{-1, f_i} = w_{f_i, j} = \exp\left\{-\frac{d(e_{f_i}, e_j)}{d(e_{f_i}, e_j)}\right\} \\ \text{if } (e_{f_i}, e_j) \text{ satisfy condition 2.} \\ a_{f_i, f_i} = -\sum w_{f_i, f_j} \\ a_{f_i, f_j} = 0 \quad \text{otherwise} \end{cases} \quad (6)$$

149 $\bar{d}(e_{f_i}, e_{f_j})$ is the average distance of all recorded distances.150 **Condition 1:** if e_{f_i} and e_{f_j} are in the same face, and all of them
151 are the folding edge.152 **Condition 2:** if e_{f_i} and e_j are in the same face, one of them e_{f_i} is
153 the folding edge, and e_j is a cutting edge in the same face with e_{f_i} .154 We now implement method 3 as we explained, but we can't find the
155 reason why this method works best, we can't find any reason to
156 support this implementation.157 **3.3.4 Method 3-1**158 The dimension of Laplacian is the sum of folding edges' size and
159 cutting edges' size which are in the same face with folding edges.160 **3.3.5 Method 3-2**161 The dimension of Laplacian is $n_f + 1$, n_f is the number of folding
162 edges. This method is mean to keep the original relations between
163 folding edges as we incorrectly set the weight of between the last
164 folding edge and any other edge, so we use the added one row and
165 column to save some covered distance. Figure 4 shows an example
166 of initial distance saved in Laplacian matrix.167 **3.3.6 Method 3-3**168 Compared with method 3-2, we only set the distance between all
169 folding edges as ∞ to observe the influence of last column and row
170 on the corresponding 3D realization.

Face Order:		Fold Edge:
0:	2 0 1	4, 8, 11
1:	1 3 4	
2:	6 4 5	
3:	5 7 8	
4:	8 9 10	
5:	12 10 11	
6:	11 13 14	
7:	16 14 15	
8:	15 17 18	
9:	13 19 20	
10:	19 21 22	
11:	21 23 24	

Method 3:	
inf	inf
inf	(4,5)
inf	(8,10)
(4,5)	(8,10)

Method 3-2	
inf	inf
inf	(4,5)
inf	(8,10)
inf	(11,14)
(4,5)	(8,10)

Figure 4: An example shows the initial distance between edge pair of Laplacian matrix by method 3 and 3-2.171 **3.3.7 Method 3-4**172 We construct the similar $n \times n$ Laplacian using all edges as its
173 dimension as Method 3-3, to see the influence of last column and
174 row, n is the number of all edges.175 **3.3.8 Method 3-5**176 We construct the $n_f \times n_f$ Laplacian matrix using random value, and
177 we put 50 and n_f values into the matrix to see the difference. Note
178 that cause the matrix is randomly generated, so the result performs
179 good and bad sometimes.180 Secondly, we calculate K eigenfunctions of A corresponding to the
181 smallest magnitudes of K eigenvalues as Φ for this mesh. (We now
182 use “scipy.sparse.linalg.eigs” in python to solve this problem. It
183 seems that it is also use “ARPACK” routines as backend the same as
184 other solvers. We choose “SM” mode to make the solver to choose
185 eigenvalues with smallest magnitudes)

	folding edge	edge
box_001	20	83
box_002	168	1288
box_004	59	764
box_005	94	950

Table 1: Edge size of boxes186 **3.4 Choice of Features**187 We try not to design handcraft features to avoid the loss of in-
188 formation during feature extraction. Therefore, we use the co-
189 ordinates of vertices from flat meshes as feature functions. For
190 each edge, there is two vertices at each end and two dimension
191 for each vertices in flat meshes, which defines the feature tensor
192 as $(X_{v_0}, Y_{v_0}, X_{v_1}, Y_{v_1})$ for a input mesh.193 **4 Methods**194 **5 Experiments**

195 We now describe the experimental part of our methods.

196 **5.1 DataBase**

197 To our knowledge, the problem we need to solve is new, thus we
 198 have not found any related database. As a result, we built our
 199 database following a flow as Figure 5.

200 For one example as shown in Figure 5(a), we collect the planar lay-
 201 out from designers, then we transfer the design into a flat triangular
 202 mesh, and finally manually fold this triangular mesh into a 3D real-
 203 alization.

204 In the end, we have 51 example pairs where each includes a flat
 205 triangular mesh and its corresponding 3D realization.

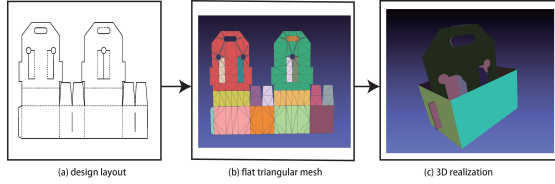


Figure 5: Take a design layout named *box_004* as an example, we collect it from designers, then we convert it to a flat triangular mesh(b), which can finally import to the interface (c) to manually assign angles to each folding edge to get the folded 3D realization.

206 **5.2 TrainingData**

207 From the database, we extract the ground truth angle as the dihedral
 208 angle between front side of two faces.

209 **5.3 Implement Details**

210 Given a flat mesh $\mathcal{M} = (\mathcal{V}, \mathcal{N}, \mathcal{E}, \mathcal{P}, \mathcal{F})$, where

- 211 • for each vertex $v_i \in \mathcal{V}$, $v_z = 0$.
- 212 • for each normal $\mathbf{n}_i \in \mathcal{N}$, $\mathbf{n}_i = (0, 0, 1)$.
- 213 • for each edge $e_i \in \mathcal{E}$, it has a label denotes the line is dash or
 214 solid.
- 215 • for each plane $p_i \in \mathcal{P}$, it is a minimum rigid polygon.
- 216 • for each triangular face $f \in \mathcal{F}$, we know $f_i \in p_j$.

217 We need to learn angles $\mathcal{A} = \{\alpha_i\}$ of the corresponding edges
 218 $\mathcal{E} = \{e_i\}$, angle α_i means the dihedral angle between front side of
 219 two faces sharing edge e_i . There is some constraints on \mathcal{A} :

- 220 • **Constrain 1** $\alpha_i = \alpha_j$ if e_i and e_j are adjacent and parallelled,
 221 also they are in the same plane.??????(how to define)
- 222 • **Constrain 2** $\alpha_i = \pi$ if e_i is inside the plane.??????(how to
 223 define)

224 The first constrain means that when two edge are on the same fold
 225 edge between two faces, they have the same fold angle. While if
 226 edges are inside the plane, the fold angle is always π .

227 We compute the mask of each edge to denote whether the edge is
 228 the folding edge or inside the plane, then we add these two con-
 229 straints to the 3D realization according to the mask.

230 Through \mathcal{A} , we can compute the new coordinates of each face
 231 which rotates around the edge e_i to angle α_i (need to modify). This
 232 just fits the physical problem of folding boxes.

233 Finally we can get the corresponding 3D realization $\hat{\mathcal{M}} =$
 234 $\{\hat{\mathcal{V}}, \hat{\mathcal{N}}, \mathcal{E}, \mathcal{P}, \mathcal{F}\}$, where $\hat{\mathcal{V}}$ and $\hat{\mathcal{N}}$ is the new computed value of
 235 vertices and normals.

236 **5.4 Results**

237 Comparison among three different constructions of Laplacian ma-
 238 trix illustrated in Section 3.3.

239 **6 User Study**

240 **7 Conclusion**

241 **Acknowledgements**

242 To all.

243 **References**

- 244 BIEDL, T. C., AND GEN, B. 2004. When can a graph form an
 245 orthogonal polyhedron? 100–102.
- 246 BIEDL, T., LUBIW, A., AND SUN, J. 2005. When can a net fold
 247 to a polyhedron? *Comput. Geom. Theory Appl.* 31, 3 (June),
 248 207–218.
- 249 CAO, L., LIU, J., AND TANG, X. 2005. 3d object reconstruction
 250 from a single 2d line drawing without hidden lines. In *Proceed-
 251 ings of the Tenth IEEE International Conference on Computer
 252 Vision (ICCV'05) Volume 1 - Volume 01*, IEEE Computer Soci-
 253 ety, Washington, DC, USA, ICCV '05, 272–277.
- 254 DAI, J. S., AND JONES, J. R. 1999. Mobility in metamorphic
 255 mechanisms of foldable/erectable kinds. *Journal of Mechanical
 256 Design* 121, 3, 375–382.
- 257 DEMAINE, E. D., AND O'ROURKE, J. 2010. A survey of folding
 258 and unfolding in computational geometry. In *Revised Papers
 259 from the Japanese Conference on Discrete and Computational
 260 Geometry*, 258–266.
- 261 KANADE, T. 1980. A theory of origami world. *Artificial Intelli-
 262 gence* 13, 3, 279 – 311.
- 263 LE, S. N., LEOW, S.-J., LE-NGUYEN, T.-V., RUIZ, C., AND
 264 LOW, K.-L. 2014. Surface and contour-preserving origamic
 265 architecture paper pop-ups. *IEEE Transactions on Visualization
 266 and Computer Graphics* 20, 2 (Feb.), 276–288.
- 267 LECLERC, Y. G., AND FISCHLER, M. A. 1992. An optimiza-
 268 tion-based approach to the interpretation of single line drawings as
 269 3d wire frames. *International Journal of Computer Vision* 9, 2,
 270 113–136.
- 271 LEVY, B. 2006. Laplace-beltrami eigenfunctions towards an algo-
 272 rithm that "understands" geometry. In *Proceedings of the IEEE
 273 International Conference on Shape Modeling and Applications
 274 2006*, IEEE Computer Society, Washington, DC, USA, SMI '06,
 275 13–.
- 276 LI, X.-Y., SHEN, C.-H., HUANG, S.-S., JU, T., AND HU, S.-M.
 277 2010. Popup: Automatic paper architectures from 3d models.
 278 In *ACM SIGGRAPH 2010 Papers*, ACM, New York, NY, USA,
 279 SIGGRAPH '10, 111:1–111:9.
- 280 LI, X.-Y., JU, T., GU, Y., AND HU, S.-M. 2011. A geometric
 281 study of v-style pop-ups: Theories and algorithms. In *ACM SIG-*

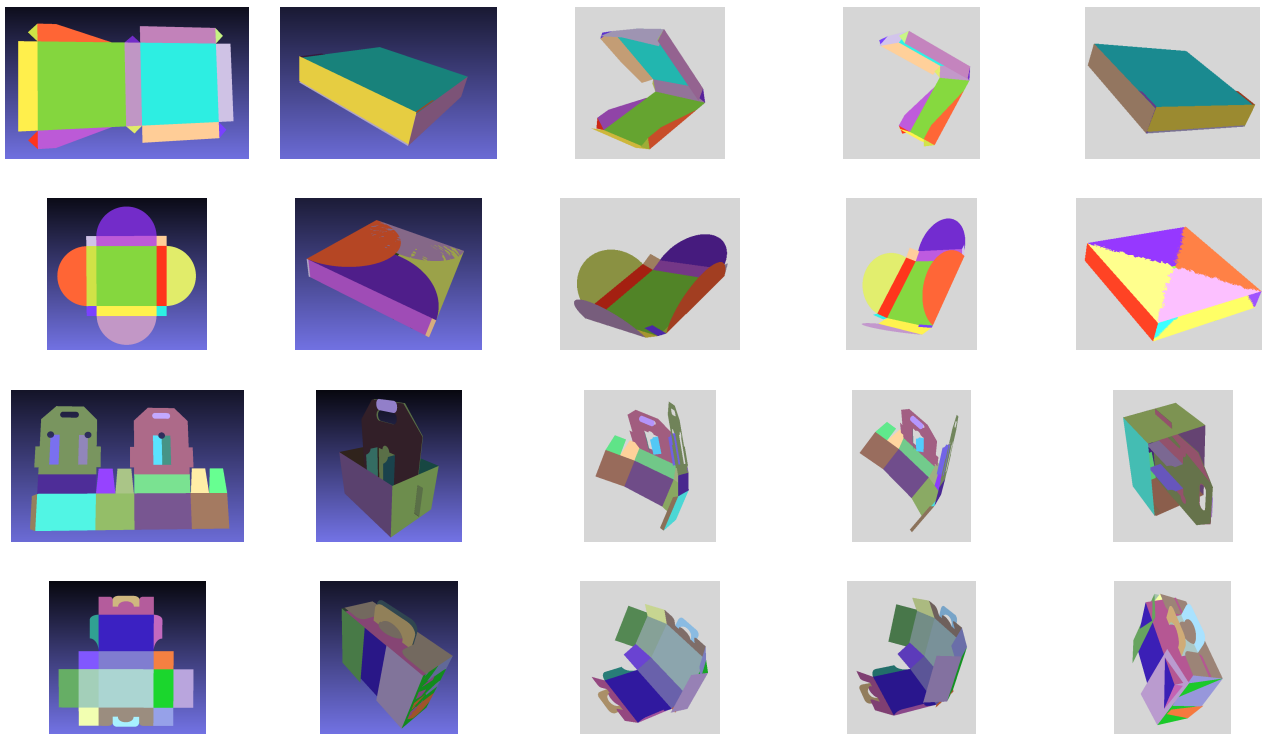


Figure 6: input, output, and method 1, 2, 3. All use $\min(60, n-2)$ coefficients, and add constrain 1 and 2

282 *GRAPH 2011 Papers*, ACM, New York, NY, USA, SIGGRAPH
 283 '11, 98:1–98:10.

284 LUBIW, A. 1996. When can a polygon fold to a polytope? *Dept.comput.sci.smith College*.

285 MARILL, T. 1991. Emulating the human interpretation of line-
 286 drawings as three-dimensional objects. *Int. J. Comput. Vision* 6,
 288 2 (June), 147–161.

289 MARILL, T. 1992. Why do we see three-dimensional objects?

290 O'Rourke, J. 2000. Folding and unfolding in computational
 291 geometry. In *Revised Papers from the Japanese Conference on*
 292 *Discrete and Computational Geometry*, Springer-Verlag, Lon-
 293 don, UK, UK, JCDCG '98, 258–266.

294 RUIZ, JR., C. R., LE, S. N., AND LOW, K.-L. 2013. Generating
 295 multi-style paper pop-up designs using 3d primitive fitting. In
 296 *SIGGRAPH Asia 2013 Technical Briefs*, ACM, New York, NY,
 297 USA, SA '13, 4:1–4:4.

298 SHOJI, K., KATO, K., AND TOYAMA, F. 2001. 3-d interpretation
 299 of single line drawings based on entropy minimization principle.

300 WIKIPEDIA, 2016. Chebychevgrblerkutzbach criterion —
 301 wikipedia, the free encyclopedia. [Online; accessed 30-
 302 September-2016].

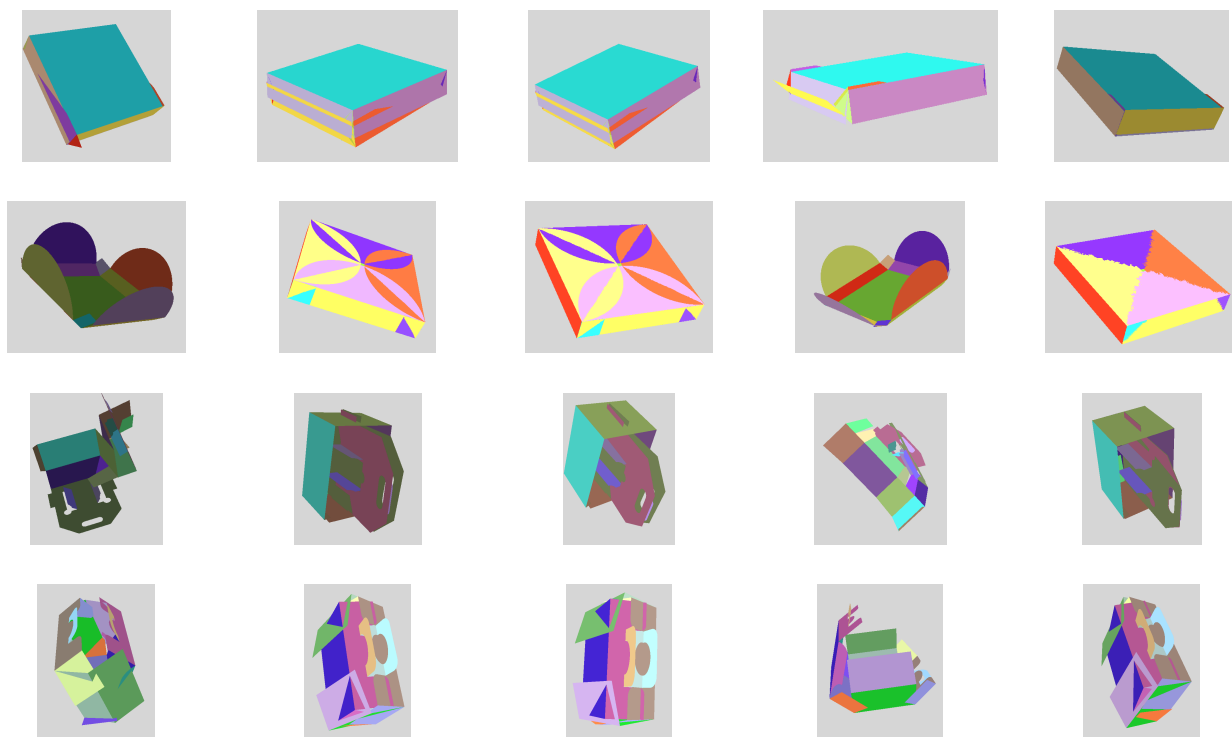


Figure 7: Method 3-1,3-2,3-3,3-4, and result by Method 3. All use $\min(60, \text{size}-2)$ coefficients, and add constrain 1,2

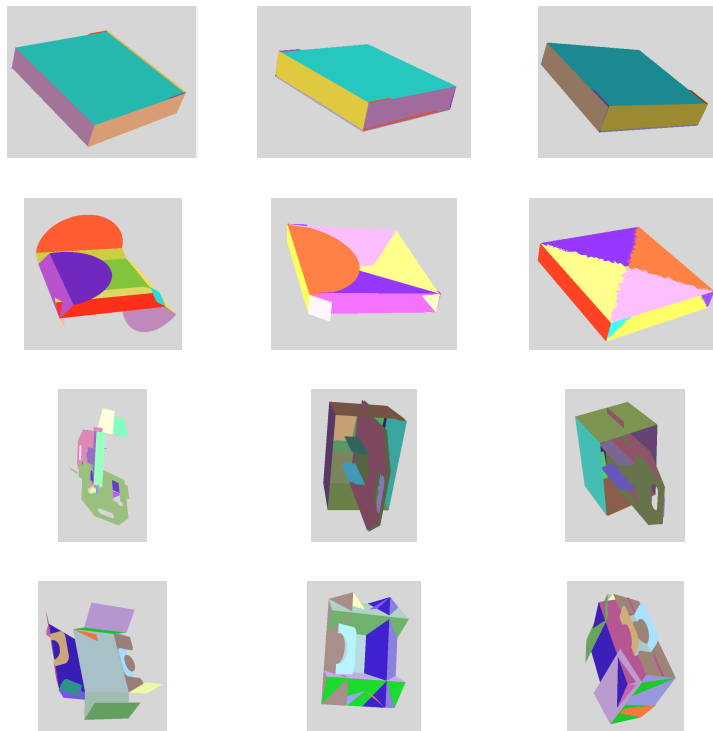


Figure 8: Method 3-5, using 50 or $2 * n_f$ values and Method 3. All use $\min(60, \text{size}-2)$ coefficients, and add constrain 1,2